Nonlinear Dyn (2017) 89:1513–1524
DOI 10.1007/s11071-017-3531-0

ORIGINAL PAPER

A swing constrained time-optimal trajectory planning strategy for double pendulum crane systems

He Chen · Yongchun Fang · Ning Sun

Received: 10 June 2016 / Accepted: 11 April 2017 / Published online: 29 April 2017
© Springer Science+Business Media Dordrecht 2017

Abstract In practice, overhead crane systems are widely used and the traditional control methods for a crane system usually treat it as a single pendulum system. However, when the hook mass cannot be ignored or the payload is too large, the crane system may behave more like a double pendulum system, which leads to the fact that traditional control methods are not suitable in this situation. In this paper, we focus on the control problem of a double pendulum crane system and propose a time-optimal trajectory planning method with the consideration of various constraints which can achieve the objectives of both accurate trolley positioning and double pendulum swing suppression. Specifically, the discrete system model is obtained using the discretization technique firstly. Then by deeply analyzing and considering a series of constraints, we formulate a quasiconvex optimization problem. After that, the bisection method is chosen to solve the obtained optimization problem with the corresponding time-optimal trajectory constructed conveniently. A tracking controller is also designed for the double pendulum crane system, which achieves proper trolley tracking performance. At last, both simulation and experimental results are included to illustrate the superior performance of the proposed trajectory planning method.

Keywords Underactuated system · Double pendulum crane · Trajectory planning · Time-optimal · Tracking control

H. Chen · Y. Fang (✉) · N. Sun
Institute of Robotics and Automatic Information System (IRAIS), Tianjin Key Laboratory of Intelligent Robotics (tjKLIR), Nankai University, Tianjin 300350, China
e-mail: fangyc@nankai.edu.cn

H. Chen
e-mail: chenh@mail.nankai.edu.cn

N. Sun
e-mail: sunn@nankai.edu.cn

1 Introduction

As an important transportation tool, overhead crane systems are widely used in factories, harbors, and so on. As a typical underactuated system [1–3], the overhead crane system is difficult to be controlled properly and due to the fact that the payload is dragged by the trolley, inappropriate operation for overhead cranes may lead to large payload swing which is very dangerous. In practice, overhead cranes are usually operated by experienced workers. However, possible operation mistakes may result in uncontrollable payload swing and even accidents. Hence, the study on automatic control design for overhead crane systems is very meaningful and useful.

Generally speaking, the control objective of the overhead crane system consists of two parts, known as fast and accurate trolley positioning, and effective payload swing suppression. However, these two parts are actually contradictory with each other, and hence, to achieve them simultaneously is of great difficulty. Recently, the control problem of overhead cranes has

attracted attentions from many researchers all over the world, with a series of control methods proposed. To simplify the control design difficulty, partial feedback linearization technique is used to obtain proper control performance in [4] and [5]. A flatness-based control method is proposed for 2-dimension overhead crane systems in [6]. In the references of [7–9], adaptive control-based methods are proposed for overhead cranes, which do not require the exact model knowledge. Utilizing the passivity theory, many energy-based control methods are proposed in [10,11], which can obtain asymptotic stability results. Considering the existence of unknown disturbance, as well as system model uncertainties, sliding mode-based control methods [12–14] are also designed for crane systems, which show great robustness. A series of open loop control methods based on the idea of input shaping are proposed for crane systems in [15–17], which need few sensors and can successfully suppress the payload swing. To deal with system constraints and the input saturation problem, model predictive control (MPC)-based methods are also proposed for overhead cranes in [18] and [19]. Low energy consumption results are also achieved for overhead crane systems by MPC-based method in [20]. In recent years, intelligent methods, including fuzzy control method [21], genetic algorithm (GA)-based method [22], neural network-based method [23], which can utilize human experience to improve the control performance, are applied to control crane systems.

Because there exists strong coupling between the trolley movement and the payload swing, more directly, we can plan a suitable trajectory for the trolley with the coupling behavior being considered. Based on this idea, a lot of trajectory planning methods have been proposed so far [24–29]. For example, Sun et al. [26] propose a phase plane-based trajectory planning method, using which a three-segment trajectory is obtained by geometric analysis in the phase plane, which can achieve the objective of swing suppression and residual swing elimination. In [27], Wu et al. propose a model conversion method, based on which three kinds of optimal trajectories, including swing-optimal, energy-optimal, and time-optimal, are presented for overhead cranes.

Though a lot of methods have been proposed for overhead crane systems, most of them need the following assumption: The payload can bee seen as a mass point. However, in some situations, for example, the payload shape is too large to be ignored, or the hook mass cannot be simply ignored, this kind of assumption is not satisfied and the overhead crane system behaves more like a double pendulum system. The dynamic behavior of a pendulum system can also be very complex, which is widely researched by many scholars [30,31]. As a result, the control performance of many controllers may be degraded or even instability results may occur, which is very dangerous. So far, there exist few methods which can deal with this problem. In [32–34], input shaping methods are extended for double pendulum cranes, which can suppress double pendulum swing. A polynomial-based trajectory planning method is proposed by Sun et al. [35], which can deal with various system constraints. Tuan et al. propose some sliding mode control-based methods for double pendulum crane systems in [36], which are testified to be robust by simulation results. An amplitude-saturated nonlinear output feedback control method [37] is presented for double pendulum crane systems, which can suppress double pendulum swing and achieve accurate trolley positioning.

Focusing on the control problem of double pendulum crane systems, we propose a time-optimal trajectory planning method in this paper, which can achieve both fast and accurate trolley positioning and double pendulum swing suppression. Specifically, by taking consideration of various system constraints, we first formulate an optimization problem, with the transportation time being the to-be-optimized function. Then a discrete system model for the double pendulum crane is presented by using the discretization technique, which can be seen as the basis to solve the obtained optimization problem. Based on this discrete model, the entire optimization problem, including optimization function and constraints, is converted into a discrete formulation. By deeply analyzing the structure of the optimization problem, it is proved that the optimization function is a quasiconvex function while the constraints are all convex, which further implies that the optimization problem is a quasiconvex problem. After that, we propose a bisection-based method to solve this problem and obtain the optimal transportation time, together with the corresponding time-optimal trajectory. Also, to make the trolley track the planned trajectory properly, a tracking controller is designed, which is proved to achieve exponential convergence results. At last, some simulation results and experimental results are included to show the great performance of the proposed method.

The rest of this paper is organized as follows: Sect. 2 introduces the double pendulum crane dynamics, as well as the control objectives. The proposed trajectory planning method, including optimization problem formulation, system transformation, optimization problem solution, and tracking controller design, is detailed in Sect. 3. To verify the performance of this method, some simulation tests, as well as experimental tests, are implemented in Sect. 4. Section 5 provides the main conclusion of this paper.

2 Problem statement

In this paper, we focus on the control problem of a double pendulum crane system, whose schematic figure is shown in Fig. 1. By some mathematical analysis and calculations, we can obtain the kinematic energy and potential energy as follows:

$$\begin{aligned} K &= \frac{1}{2}(M+m_1+m_2)\dot{x}^2 + \frac{1}{2}(m_1+m_2)l_1^2\dot{\theta}_1^2 \\ &\quad + \frac{1}{2}m_2 l_2^2\dot{\theta}_2^2 + (m_1+m2)l_1\cos\theta_1\dot{x}\dot{\theta}_1 \\ &\quad + m_2 l_2\cos\theta_2\dot{x}\dot{\theta}_2 + m_2 l_1 l_2\cos(\theta_1-\theta_2)\dot{\theta}_1\dot{\theta}_2, \\ P &= (m_1+m2)gl_1(1-\cos\theta_1) + m_2 g l_2(1-\cos\theta_2), \end{aligned}$$

where $K(t) and P(t)$ denote the kinematic and potential energies, respectively. Then, the Lagrangian function is defined as $L(t) = K(t) - P(t)$. After that, we can calculate the crane system dynamic model using the following Lagrangian equations:

$$\begin{aligned} \frac{\mathrm{d}}{\mathrm{d}t}\left(\frac{\partial L}{\partial \dot{x}}\right) - \frac{\partial L}{\partial x} &= F, \\ \frac{\mathrm{d}}{\mathrm{d}t}\left(\frac{\partial L}{\partial \dot{\theta}_1}\right) - \frac{\partial L}{\partial \theta_1} &= 0, \end{aligned}$$

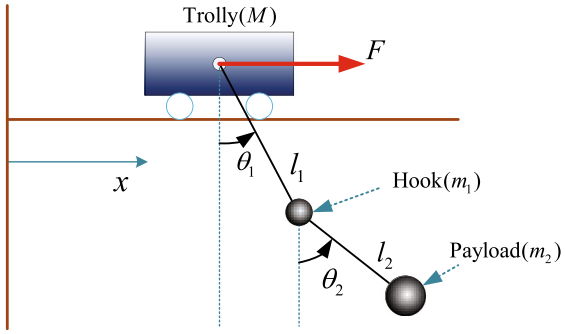

Fig. 1 Schematic figure of double pendulum crane systems

$$\frac{\mathrm{d}}{\mathrm{d}t}\left(\frac{\partial L}{\partial \dot{\theta}_2}\right) - \frac{\partial L}{\partial \theta_2} = 0,$$

which is explicitly given as

$$\begin{aligned} &(M+m_1+m_2)\ddot{x} + (m_1+m_2)l_1(\cos\theta_1\ddot{\theta}_1 - \dot{\theta}_1^2\sin\theta_1) \\ &\quad + m_2 l_2\ddot{\theta}_2\cos\theta_2 - m_2 l_2\dot{\theta}_2^2\sin\theta_2 = F, \qquad (1) \\ &(m_1+m_2)l_1\cos\theta_1\ddot{x} + (m_1+m_2)l_1^2\ddot{\theta}_1 \\ &\quad + m_2 l_1 l_2\cos(\theta_1-\theta_2)\ddot{\theta}_2 + m_2 l_1 l_2\sin(\theta_1-\theta_2)\dot{\theta}_2^2 \\ &\quad + (m_1+m_2)gl_1\sin\theta_1 = 0, \qquad (2) \\ &m_2 l_2\cos\theta_2\ddot{x} + m_2 l_1 l_2\cos(\theta_1-\theta_2)\ddot{\theta}_1 + m_2 l_2^2\ddot{\theta}_2 \\ &\quad - m_2 l_1 l_2\dot{\theta}_1^2\sin(\theta_1-\theta_2) + m_2 g l_2\sin\theta_2 = 0, \qquad (3) \end{aligned}$$

where $M, m_1, and m_2$ represent the trolley mass, the non-negligible hook mass, and the payload mass, respectively; l_1 denotes the rope length; and l_2 is the distance between centers of the hook and the payload; g represents the gravity acceleration constant. The trolley displacement is described by $x(t)$. The double pendulum swing angles, known as the hook swing angle and the payload swing angle, are expressed by $\theta_1(t)$ and $\theta_2(t)$. It is seen that $x(t), \theta_1(t), \theta_2(t)$ constitute the to-be-controlled system states. $F(t)$ is the force actuated on the trolley, which is the only control input of this system.

It is obvious that the number of control input is less than that of degrees of freedom, which clearly shows that the double pendulum system is a typical underactuated system. At the same time, due to the existence of hook swing angle, the system states of this kind of crane system are more than those of a single pendulum crane system while there is still one control input, which increases the control difficulty of this system. Like the single pendulum crane system, the control objective of the double pendulum crane consists of two parts, fast and accurate trolley positioning and double pendulum swing suppression. To achieve this objective, in this paper, we decide to plan a suitable trajectory for the trolley, with the consideration of swing suppression during the planning process. In the next section, the coupling relationship of the system states will be analyzed deeply, which is the key for trajectory planning.

3 Time-optimal trajectory planning strategy

In this section, a novel time-optimal trajectory planning strategy is proposed for the double pendulum crane system to achieve the objective of both fast and accurate

trolley positioning and effective system swing suppression. Specifically, we first formulate an optimization problem with the consideration of various constraints, by solving which we can obtain the time-optimal trolley trajectory. Then by utilizing the discretization technique, the discrete system model is obtained, based on which, the optimization problem is transformed into a discrete form. After that, the discrete optimization problem is proven to be a quasiconvex optimization problem, which is then solved by a bisection method. At last, a global time-optimal trolley trajectory is obtained, following which, the transportation process can be finished with no residual swing.

3.1 Optimization problem formulation

To obtain the time-optimal trolley trajectory, we need to formulate an optimization problem with the following constraints taken into consideration:

(1) Considering the control objective, the trolley should reach the desired position x_f from the initial position x_i within transportation time t_f, while the trolley velocity and acceleration should be equal to zero when the trolley reaches the target position. At the same time, both double pendulum swing angles ought to be zero, as well as the swing angular velocities. That is

$$\begin{aligned}
&x(0)=0, \quad \dot{x}(0)=0, \quad \ddot{x}(0)=0,\\
&x(t_f)=x_f, \quad \dot{x}(t_f)=0, \quad \ddot{x}(t_f)=0,\\
&\theta_1(0)=\theta_2(0)=0, \quad \dot{\theta}_1(0)=\dot{\theta}_2(0)=0,\\
&\theta_1(t_f)=\theta_2(t_f)=0, \quad \dot{\theta}_1(t_f)=\dot{\theta}_2(t_f)=0.
\end{aligned}$$

Without loss of generality, the initial time is chosen as zero and x_i is set as zero.

(2) Due to the actuator saturation, the trolley velocity and acceleration should be within suitable domains, in the sense that,

$$|\dot{x}(t)| \le v_{\max}, \quad |\ddot{x}(t)| \le a_{\max},$$

where $v_{\max}, a_{\max}$, respectively, denote the permitted trolley velocity and acceleration amplitudes.

(3) To ensure safety, the maximum amplitudes of double pendulum swing angles should be less than allowable values. Thus, we have the following relationship:

$$|\theta_1(t)| \le \theta_{1\max}, \quad |\theta_2(t)| \le \theta_{2\max},$$

wherein $\theta_{1\max}, \theta_{2\max}$ represent the allowed upper bounds of the double pendulum swing angles, respectively.

In summary, we can formulate an optimization problem with respect to the transportation time t_f as follows:

$$\begin{aligned}
\text{minimize} \quad & t_f\\
\text{subject to} \quad & x(0)=0, \quad \dot{x}(0)=0, \quad \ddot{x}(0)=0,\\
& x(t_f)=x_f, \quad \dot{x}(t_f)=0, \quad \ddot{x}(t_f)=0,\\
& \theta_1(0)=\theta_2(0)=0, \quad \dot{\theta}_1(0)=\dot{\theta}_2(0)=0,\\
& \theta_1(t_f)=\theta_2(t_f)=0, \quad \dot{\theta}_1(t_f)=\dot{\theta}_2(t_f)=0,\\
& |\dot{x}(t)| \le v_{\max}, \quad |\ddot{x}(t)| \le a_{\max},\\
& |\theta_1(t)| \le \theta_{1\max}, \quad |\theta_2(t)| \le \theta_{2\max}. \qquad (4)
\end{aligned}$$

3.2 System discretization

Linearizing the system dynamics shown in (1)–(3) around the equilibrium point and after some simplifications, we can obtain

$$(M+m_1+m_2)\ddot{x}+(m_1+m_2)l_1\ddot{\theta}_1+m_2l_2\ddot{\theta}_2=F, \qquad (5)$$

$$\ddot{x}+l_1\ddot{\theta}_1+\frac{m_2l_2}{m_1+m_2}\ddot{\theta}_2+g\theta_1=0, \qquad (6)$$

$$\ddot{x}+l_1\ddot{\theta}_1+l_2\ddot{\theta}_2+g\theta_2=0. \qquad (7)$$

Then after some transformations, the double pendulum swing angular accelerations can be expressed as follows:

$$\ddot{\theta}_1=-\frac{\ddot{x}}{l_1}-\frac{g(m_1+m_2)}{m_1l_1}\theta_1+\frac{gm_2}{m_1l_1}\theta_2, \qquad (8)$$

$$\ddot{\theta}_2=\frac{g(m_1+m_2)}{m_1l_2}\theta_1-\frac{g(m_1+m_2)}{m_1l_2}\theta_2. \qquad (9)$$

Treat the trolley acceleration as the system input and then (8) and (9) can be rewritten as the state-space representation:

$$\dot{\boldsymbol{\xi}}=A\boldsymbol{\xi}+\boldsymbol{B}u, \qquad (10)$$

where $u(t)$ is the system input, which is equal to the trolley acceleration $\ddot{x}(t)$; $\boldsymbol{\xi}(t) \in \mathbb{R}^{6\times1}$ denotes the full state vector defined as follows:

$$\boldsymbol{\xi}=[\,x \quad \dot{x} \quad \theta_1 \quad \dot{\theta}_1 \quad \theta_2 \quad \dot{\theta}_2\,]^T,$$

$A \in \mathbb{R}^{6\times6}$, $\boldsymbol{B} \in \mathbb{R}^{6\times1}$ represent system parameter matrices with the following expressions:

$$A = \begin{bmatrix} 0 & 1 & 0 & 0 & 0 & 0 \\ 0 & 0 & 0 & 0 & 0 & 0 \\ 0 & 0 & 0 & 1 & 0 & 0 \\ 0 & 0 & -\frac{g(m_1+m_2)}{m_1 l_1} & 0 & \frac{g m_2}{m_1 l_1} & 0 \\ 0 & 0 & 0 & 0 & 0 & 1 \\ 0 & 0 & \frac{g(m_1+m_2)}{m_1 l_2} & 0 & -\frac{g(m_1+m_2)}{m_1 l_2} & 0 \end{bmatrix},$$

$$\boldsymbol{B} = \begin{bmatrix} 0 & 1 & 0 & -1/l_1 & 0 & 0 \end{bmatrix}^T.$$

To facilitate trajectory planning, select the sample time as T, and (10) can be then discretized as follows:

$$\boldsymbol{\xi}(k+1) = A_d \boldsymbol{\xi}(k) + \boldsymbol{B}_d u(k), \tag{11}$$

where $\boldsymbol{\xi}(k)$ and $u(k)$ denote the system state vector and the system input at time k, respectively; $A_d and \boldsymbol{B}_d$ represent the discrete system parameter matrices which can be calculated as

$$A_d = \exp(AT), \quad \boldsymbol{B}_d = \int_0^T \exp(AT)\mathrm{d}t\, \boldsymbol{B}, \tag{12}$$

where $\exp(*)$ denotes the natural exponential function.

Based on the discrete system model (11), the original optimization problem can be converted into a discrete structure as follows:

$$\begin{aligned} &\text{minimize} && k_f \\ &\text{subject to} && \boldsymbol{\xi}(0) = \boldsymbol{\xi}_i, \quad \boldsymbol{\xi}(k_f) = \boldsymbol{\xi}_f, \\ &&& u(0) = 0, u(k_f) = 0, \\ &&& |u(k)| \le a_{\max}, \quad |\boldsymbol{E}_v \boldsymbol{\xi}(k)| < v_{\max}, \\ &&& |\boldsymbol{E}_{t1} \boldsymbol{\xi}(k)| < \theta_{1\max}, \quad |\boldsymbol{E}_{t2} \boldsymbol{\xi}(k)| < \theta_{3\max}, \end{aligned} \tag{13}$$

where k_f represents the to-be-optimized discrete time variable and we have the following relationship:

$$t_f = k_f T.$$

$\boldsymbol{\xi}_i, \boldsymbol{\xi}_f \in \mathbb{R}^{6\times1}$ denote the initial and target position system state vectors, respectively, which are defined as follows:

$$\boldsymbol{\xi}_i = [0 \quad 0 \quad 0 \quad 0 \quad 0 \quad 0]^T,$$
$$\boldsymbol{\xi}_f = [x_f \quad 0 \quad 0 \quad 0 \quad 0 \quad 0]^T,$$

$\boldsymbol{E}_v, \boldsymbol{E}_{t1}, \boldsymbol{E}_{t2} \in \mathbb{R}^{1\times6}$ are auxiliary matrices with the following expressions:

$$\boldsymbol{E}_v = [0 \quad 1 \quad 0 \quad 0 \quad 0 \quad 0],$$
$$\boldsymbol{E}_{t1} = [0 \quad 0 \quad 1 \quad 0 \quad 0 \quad 0],$$
$$\boldsymbol{E}_{t2} = [0 \quad 0 \quad 0 \quad 0 \quad 1 \quad 0].$$

Next, we will solve the optimization problem to construct the optimal trolley trajectory.

3.3 Optimization problem analysis and solution

At first, an auxiliary function should be formulated to describe the transportation time k_f. Choose $K \in \mathbb{R}^+$ as a sufficiently large integer and the control objective of the overhead crane system can be achieved by selecting proper control input sequence $u(0), u(1), \ldots, u(K)$ to drive (11) from the initial state to the target state with constraints satisfied. Considering the transportation time k_f, it is obvious that the following relationship is satisfied:

$$k_f \in \{k_f | \boldsymbol{\xi}(k_f) = \boldsymbol{\xi}_f, u(k) = 0 \quad \text{for} \quad k_f \le k \le K\}. \tag{14}$$

Based on (14), the optimal transportation time can be expressed as a function with respect to the control input sequence as follows:

$$\begin{aligned} \phi(u(0), \ldots, u(K)) = \min\{k_f | \boldsymbol{\xi}(k_f) = \boldsymbol{\xi}_f, \\ u(k) = 0 \quad \text{for} \quad k_f \le k \le K\}. \end{aligned} \tag{15}$$

Next we need to prove that the to-be-optimized function $\phi(u(0), \ldots, u(K))$ is a quasiconvex function with the following definition:

Definition 1 Quasiconvex function [38]: a function $f : \mathbb{R}^n \to \mathbb{R}$ is called *quansiconvex* (or *unimodal*) if its domain and all its sublevel sets

$$S_\alpha = \{x \in dom\ f | f(x) \le \alpha\},$$

for $\alpha \in \mathbb{R}$, are convex.

For the function ϕ, giving an arbitrary value $\alpha \in \mathbb{Z}^+$, the sublevel set can be expressed as follows:

$$\begin{aligned} S_\alpha = \{(u(0), \ldots, u(K)) | \boldsymbol{\xi}(\alpha) = \boldsymbol{\xi}_f, \\ u(k) = 0 \text{ for } \alpha \le k \le K\}. \end{aligned} \tag{16}$$

Now consider the discrete system model shown in (11). Utilizing the integration technique, the system state at time k can be expressed in the following manner:

$$\begin{aligned}\boldsymbol{\xi}(k) &= A_d^k \boldsymbol{\xi}_i + A_d^{k-1}\boldsymbol{B}_d u(0) + \cdots + \boldsymbol{B}_d u(k-1) \\ &= A_d^k \boldsymbol{\xi}_i + \sum_{j=1}^{k} A_d^{k-j}\boldsymbol{B}_d u(j-1). \end{aligned} \tag{17}$$

Then using (17), the sublevel set (16) can be converted into the following expressions:

$$\begin{aligned} S_\alpha = \Big\{ &(u(0), \ldots, u(K)) | u(k) = 0 \text{ for } \alpha \le k \le K, \\ &A_d^\alpha \boldsymbol{\xi}_i + \sum_{j=1}^{\alpha} A_d^{\alpha-j}\boldsymbol{B}_d u(j-1) = \boldsymbol{\xi}_f \Big\}. \end{aligned} \tag{18}$$

After some analysis, it is seen that S_α is affine with respect to the control input sequence, implying that any line with two distinct points in S_α lies in the plane S_α, and we can further conclude that S_α is also convex, which indicates that $\phi(u(0), \ldots, u(K))$ is a quasiconvex function based on Definition 1.

Next, utilizing (17), the constraints in (13) can all be converted into the following expressions:

$$\boldsymbol{\xi}(0) = \boldsymbol{\xi}_i, u(0) = u(k_f) = 0, \tag{19}$$

$$A_d^{k_f} \boldsymbol{\xi}_i + \sum_{j=1}^{k_f} A_d^{k_f-j}\boldsymbol{B}_d u(j-1) = \boldsymbol{\xi}_f, \tag{20}$$

$$\boldsymbol{E}_v A_d^k \boldsymbol{\xi}_i + \boldsymbol{E}_v \sum_{j=1}^{k} A_d^{k-j}\boldsymbol{B}_d u(j-1) \le v_{\max}, \tag{21}$$

$$-\boldsymbol{E}_v A_d^k \boldsymbol{\xi}_i - \boldsymbol{E}_v \sum_{j=1}^{k} A_d^{k-j}\boldsymbol{B}_d u(j-1) \le v_{\max}, \tag{22}$$

$$\boldsymbol{E}_{t1} A_d^k \boldsymbol{\xi}_i + \boldsymbol{E}_{t1} \sum_{j=1}^{k} A_d^{k-j}\boldsymbol{B}_d u(j-1) \le \theta_{1\max}, \tag{23}$$

$$-\boldsymbol{E}_{t1} A_d^k \boldsymbol{\xi}_i - \boldsymbol{E}_{t1} \sum_{j=1}^{k} A_d^{k-j}\boldsymbol{B}_d u(j-1) \le \theta_{1\max}, \tag{24}$$

$$\boldsymbol{E}_{t2} A_d^k \boldsymbol{\xi}_i + \boldsymbol{E}_{t2} \sum_{j=1}^{k} A_d^{k-j}\boldsymbol{B}_d u(j-1) \le \theta_{2\max}, \tag{25}$$

$$-\boldsymbol{E}_{t2} A_d^k \boldsymbol{\xi}_i - \boldsymbol{E}_{t2} \sum_{j=1}^{k} A_d^{k-j}\boldsymbol{B}_d u(j-1) \le \theta_{2\max}, \tag{26}$$

$$u(k) \le a_{\max}, -u(k) \le a_{\max}, \tag{27}$$

which are all linear constraints with respect to the control input sequence, implying that the constraints of the optimization problem are all convex with respect to the control input sequence. In summary, we can find that the to-be-optimized function is a quasiconvex function while the corresponding constraints are all convex, which conforms the request of the following definition:

Definition 2 Quasiconvex optimization [38]: A quasiconvex optimization problem has the standard form

$$\begin{aligned} \text{minimize} \quad & f_0(x) \\ \text{subject to} \quad & f_i(x) \le 0, \quad i = i, \ldots, m \\ & Ax = b, \end{aligned} \tag{28}$$

where the inequality constraint function $f_1, \ldots, f_m$ are convex, and the objective f_0 is quasiconvex.

Based on Definition 2, it is concluded that (13) is a quasiconvex optimization problem which can be reformulated as:

$$\begin{aligned} \text{minimize} \quad & \phi(u(0), \ldots, u(K)) \\ \text{subject to} \quad & \boldsymbol{\xi}(0) = \boldsymbol{\xi}_i, \\ & A_d^{k_f} \boldsymbol{\xi}_i + \sum_{j=1}^{k_f} A_d^{k_f-j}\boldsymbol{B}_d u(j-1) = \boldsymbol{\xi}_f, \\ & u(k) = 0, \quad \text{for} \quad k_f \le k \le K, \\ & (21)-(27), \quad \text{for} \quad 0 \le k \le K. \end{aligned} \tag{29}$$

As stated in [38], quasiconvex optimization problems, such as (29), can be solved by the bisection method with the globally optimal solution being obtained. To describe the detailed process of solving (29), we include Algorithm 1 to show the corresponding pseudo codes of the bisection method, wherein k_a, k_b, respectively, denote the lower and upper bounds of the optimal time which are changing in every loop until the optimal time k_f^* is found. Using Algorithm 1, we can solve the optimization problem with the minimum transportation time, as well as the corresponding optimal control input sequence $u^*(k)$, $0 \le k \le k_f^*$, being obtained. Then by utilizing this sequence and (17), we can calculate the system state trajectories and finish the time-optimal trajectory planning process.

Remark 1 After the above analysis, it is seen that a series of feasibility problems need to be solved to find the feasible control sequence $u(0), \ldots, u(K)$ with (21)–(27) being satisfied. Because the constraints are all linear with respect to the control input sequence, this

Algorithm 1 Solving problem (29) by bisection-based method

Input: $\boldsymbol{\xi}_i, \boldsymbol{\xi}_f, k_a, k_b, A_d, B_d, v_{\max}, \theta_{1\max}, \theta_{2\max}, u_{\max}$.
Output: $k_f^*,\ u^*(k), k = 1, \ldots, k_f^*$.

```
while k_a < k_b do
set: k_m = (k_a + k_b)/2
solve the feasibility problem
    Find u(k), k = 1, ..., k_m
    subject to
    A_d^{k_f} ξ_i + Σ_{j=1}^{k_f} A_d^{k_f - j} B_d u(j-1) = ξ_f,
    (21)–(27), for 0 ≤ k ≤ k_m.
if the problem is feasible then
k_b = k_m
else
k_a = k_m
end if
end while
k_f^* = k_a,  u^*(k) = u(k),  k = 1, ..., k_f^*
```

feasibility problem is essentially a linear programming problem. In fact, there exist a lot of linear programming methods to solve this kind of problem, which are included in many optimization software toolboxes.

3.4 Tracking controller design

To make the trolley go along the planned trajectory, an effective tracking controller is needed. Consider the linearized system dynamics in (5)–(7). Using (5) and (6), we can obtain the following relationship:

$$M\ddot{x} - g(m_1 + m_2)\theta_1 = F. \tag{30}$$

Define the tracking error as follows

$$e = x - x_r, \tag{31}$$

where $e(t)$ denotes the trolley tracking error and $x_r(t)$ represents the planned optimal trolley trajectory, which can be obtained by the method in the previous section. Differentiate (31) with respect to time twice and the following relationship is obtained:

$$\ddot{e} = \ddot{x} - \ddot{x}_r, \tag{32}$$

where $\ddot{x}_r(t)$ denotes the second-order time derivative of the planned trajectory $x_r(t)$. Based on (30) and (32), we can present the following tracking error system:

$$M\ddot{e} = F + g(m_1 + m_2)\theta_1 - m\ddot{x}_r. \tag{33}$$

Then, we can design the tracking controller as follows:

$$F = M\ddot{x}_r - g(m_1 + m_2)\theta_1 - Mk_p e - Mk_d\dot{e}, \tag{34}$$

wherein $k_p, k_d \in \mathbb{R}^+$ denote positive control gains. Substitute (34) into (33) and the following closed-loop system is obtained:

$$\ddot{e} + k_d\dot{e} + k_p e = 0. \tag{35}$$

Utilizing Routh–Hurwitz stability theory and after some mathematical calculations, it can be proved that this closed-loop system is exponentially stable when the control gains satisfy the conditions of $k_p > 0, k_d > 0$, which means that $e(t), \dot{e}(t), \ddot{e}(t) \to 0$. In summary, we can conclude that the designed tracking controller can drive the trolley to the desired position along the planned optimal trajectory.

It should be noted and emphasized that during the tracking controller design process, the assumption of known model knowledge, as well as negligible external disturbances, has been used. To obtain better robustness, we will try to design robust control strategies in our future work.

Remark 2 The control gains of the proposed tracking controller are selected by trail and error. In general, by utilizing Routh-Hurwitz stability theory, we can select k_p, k_d to obtain exponential results. To obtain better tracking performance, after numerous simulation and experimental tests, we have summarized the following guidelines. The larger the k_p is, the shorter the convergence time will be. However, severe oscillation may occur for $x(t), \theta_1(t)$ and $\theta_2(t)$, if k_p is selected too large. The larger the k_d is, the longer the convergence time will be; on the other hand, less oscillation may occur.

Remark 3 It should be noted that even though the considered double pendulum system is linearized, it is still more accurate than the single one to describe the real behavior of cranes in some situations, when the shapes of payloads need to be considered or the hook mass cannot be ignored. Additionally, for the trajectory planning methods [15,16,26,27], linearization is a widely accepted practice to deal with the high coupling and simplify mathematical analysis. Even though the system model is linearized, the double pendulum behavior still exists in this model, which implies that this model

can still describe the real behavior of cranes in some situations. Therefore, the linearized model is adopted to facilitate the description. Generally speaking, model uncertainties and disturbances are usually ignored for trajectory planning methods, since this kind of method is an open loop control strategy, which is suitable in situations without severe disturbances. On the other hand, please kindly note that there exist some regulation/stabilization methods for overhead crane systems, which use system states/outputs as feedback and show great robustness. For complex working condition with various disturbances, tracking controllers with specific consideration on disturbance rejection can be successfully combined with the designed trajectory planner, so as to achieve satisfactory control performance.

4 Simulation and experiments

In this section, some simulation and experimental tests of the proposed method are implemented to illustrate the satisfactory performance.

4.1 Simulation results

To verify the performance of the proposed time-optimal trajectory planning method, we implement some simulation tests in the environment of MATLAB/Simulink. In particular, the time-optimal trajectory is first obtained by some off-line calculations and then tested to show the effectiveness.

In this paper, to solve the feasibility problem in the bisection method, we use CVX, a package for specifying and solving convex programs [39,40]. In the simulation, the system parameters are selected as follows:

$$M = 6.5\,\text{kg}, \quad m_1 = 2.0\,\text{kg}, \quad m_2 = 0.5\,\text{kg},$$
$$l_1 = 0.53\,\text{m}, \quad l_2 = 0.4\,\text{m}, \quad g = 9.8\ \text{m/s}^2,$$

which are the same with those of the self-built double pendulum crane test bed. The sample time for the discrete system is $T = 0.005$ s. The target position for the trolley is set as $x_f = 0.6$ m, and the system constraints are chosen as

$$a_{\max} = 0.15\,\text{m/s}^2, \quad v_{\max} = 0.5\,\text{m/s},$$
$$\theta_{1\,\max} = 2\,\text{deg}, \quad \theta_{2\,\max} = 2\,\text{deg}.$$

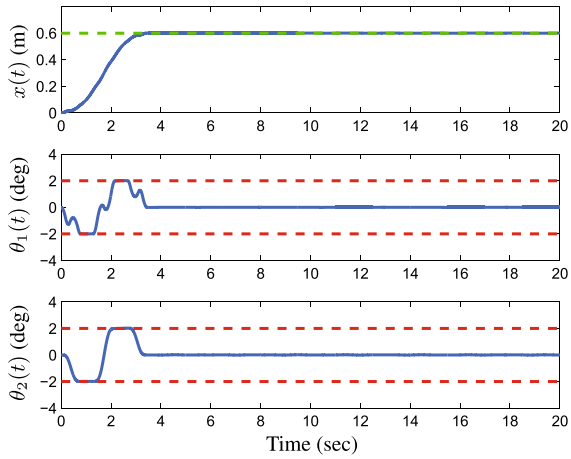

Fig. 2 Simulation results of the proposed trajectory planning method (trolley position and first- and second-order swing angles). *Solid line* simulation results; *red dashed line* swing angle constraints $\theta_{1\,\max} = \theta_{2\,\max} = 2$ deg; *green dashed line* trolley target position $x_d = 0.6$ m. (Color figure online)

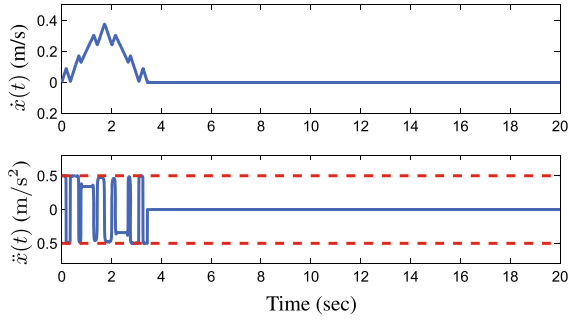

Fig. 3 Simulation results of the proposed trajectory planning method (trolley velocity and acceleration). *Solid line* simulation results; *red dashed line* trolley acceleration constraint $a_{\max} = 0.15\,\text{m/s}^2$. (Color figure online)

For the bisection method, K, k_a, k_b are set as $k_a = 200$, $k_b = K = 1000$. After some off-line calculations, we can obtain the optimal k_f^* as $k_f^* = 689$, as well as the corresponding optimal control input sequence.

The simulation results are shown in Figs. 2 and 3. We can find that when the trolley goes along the obtained optimal trajectory, it takes $t_f^* = k_f^* T = 3.445$ s to reach the target position and there is no residual swing for the double pendulum swing angles. At the same time, it is found that all system constraints, including double pendulum swing constraints, trolley velocity constraint, and trolley acceleration constraint, are satisfied during the entire transportation process. In summary, it is concluded that the proposed trajectory planning method

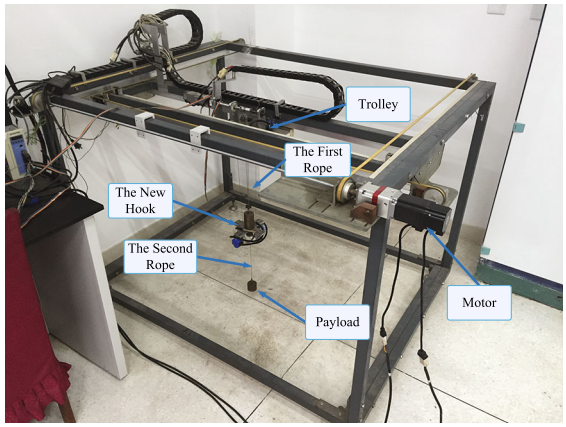

Fig. 4 Main mechanical structure of the self-built double pendulum crane test bed

can achieve the control objectives of fast and accurate trolley positioning and double pendulum swing suppression, while it can also deal with various system constraints to ensure safety.

4.2 Experimental results

To implement the proposed method, a self-built test bed, whose mechanical structure is shown in Fig. 4, is utilized. The first rope and the second rope in this figure correspond to l_1, l_2 of the system dynamics. Different from the traditional crane test bed, to measure the double pendulum swing angle in real-time, the traditional hook has been replaced by a new hook of a special structure designed by us, which is shown in Fig. 4. In particular, the payload is connected to the new hook by a massless rope. When the payload swings around the hook, a structure of a half arc fixed on the hook is driven to rotate at the same time. Using the encoder equipped at the rotating shaft of the arc, the double pendulum swing with respect to the hook can be measured in real time. For the control system, the real-time control command is calculated by MATLAB/Simulink Real-Time Windows Target and then transferred to the hardware by a motion control board, which can also obtain the measured data by encoders. For the self-built crane test bed, the sample time is determined by the chosen control board, which is set as 5 ms.

To show the great performance of the proposed method, we have chosen two comparative methods, the sliding mode method from [36] and the linear quadratic regulator (LQR) method. The system parameters of the experiment test bed can be measured, which are the same with those in simulation tests. Also, for all these three methods, the trolley target position is selected as $x_f = 0.6\,\mathrm{m}$.

Due to the space limitation, the expression of the sliding mode controller is omitted here, and we only include the selected control gains as follows:

$$K = 30, \quad \lambda = 1, \quad \alpha = 2, \quad \beta = -0.2.$$

For the LQR method, the controller expression is provided as:

$$F_L = -k_1(x - x_f) - k_2\dot{x} - k_3\theta_1 - k_4\dot{\theta}_1 - k_5\theta_2 - k_6\dot{\theta}_2,$$

and the cost function of this method is defined as

$$J = \int_0^\infty (\boldsymbol{\zeta}^{\mathrm{T}} Q \boldsymbol{\zeta} + R F_L^2)\mathrm{d}t,$$

wherein $\boldsymbol{\zeta} \in \mathbb{R}^{6\times 1}$ is defined as follows:

$$\boldsymbol{\zeta} = [\, e_l(t) \quad \dot{e}_l(t) \quad \theta_1(t) \quad \dot{\theta}_1(t) \quad \theta_2(t) \quad \dot{\theta}_2(t) \,]^T,$$

$e_l(t)$ denotes the trolley positioning error defined as $e_l(t) = x(t) - x_f$. $Q \in \mathbb{R}^{6\times 6}$, $R \in \mathbb{R}$ are auxiliary matrices selected as

$$Q = \mathrm{diag}\{180, 1, 100, 1, 100, 1\}, \quad R = 0.05.$$

Then, by using MATLAB, the control gains are calculated as

$$k_1 = 60.00, \quad k_2 = 45.46, \quad k_3 = -95.78,$$
$$k_4 = -5.98, \quad k_5 = 17.41, \quad k_6 = -4.17.$$

For the proposed method, the system constraints are selected the same with those in the simulation test, while the parameters of the bisection method are also the same. Thus, the obtained time-optimal trajectory is just the one in the simulation tests. On the other hand, for the designed tracking controller, the control gains are selected as $k_p = 120$, $k_d = 80$.

In the experimental environment, there exists friction between the trolley and the rail, and to obtain proper control performance, it needs to be well compensated. The expression of the friction can be obtained using the modeling and identification technique, which

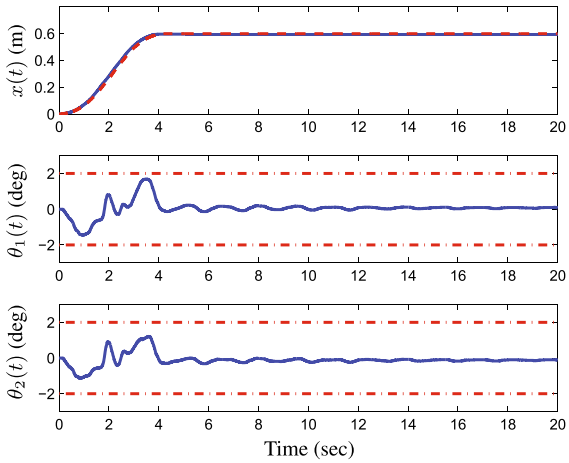

Fig. 5 Results for the proposed method. *Solid line* experimental results; *dashed line* the planned time-optimal trajectory; *dotted-dashed line* the swing angle constraints $\theta_{1\max} = \theta_{2\max} = 2\,\text{deg}$

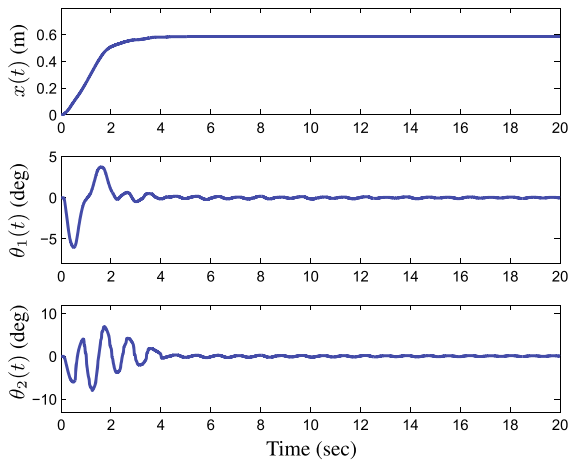

Fig. 6 Results for the sliding mode control method. *Solid line* experimental results

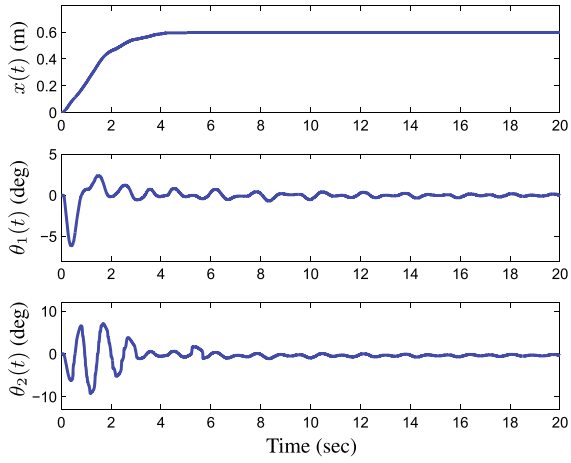

Fig. 7 Results for the LQR method. *Solid line* experimental results

is approximately described by the following model [41]:

$$F_f = F_{f1}\tanh(\epsilon_x \dot{x}) + F_{f2}|\dot{x}|\dot{x},$$

where $\dot{x}(t)$ is the trolley velocity and $F_{f1}, F_{f2}, \epsilon_x \in \mathbb{R}$ denote the friction related parameters which can be identified by a series of off-line experiments and data fitting. Then, it is summarized that utilizing the obtained model, the friction can be approximately compensated, which is widely used in crane control related papers [10,19]. Additionally, from the experimental results of the proposed method, we can conclude that using this compensation method, satisfactory tracking performance is obtained, which further shows the effectiveness of the constructed friction model.

The experimental results of the proposed method, the SMC method, and the LQR method are shown in Figs. 5, 6, and 7. Also, some quantified results are included in Table 1. From these figures and the table, it is seen that among all three methods, the time cost of the proposed method is the least, which demonstrates the time-optimal property of the proposed method. On the other hand, for the proposed method, we can find that the first and second pendulum swing angles are both within permitted domains, which implies that the given swing angle constraints are satisfied. However, the comparative methods cannot ensure the swing angle constraints, implying that these methods may be inapplicable in some situations. In summary, we can conclude that the proposed method can achieve satisfactory performance.

By comparing Figs. 2 and 5, it is seen that some differences exist between simulation and experimental results of the proposed method. Generally speaking, for the same control method, numerical simulation and experimental results are usually different due to the existence of such factors as friction, dead-zone, hysteresis, and so on [42–44]. In particular, since unavoidable disturbance exists, the experimental results in this paper are not exactly the same with the simulation ones, which can be seen as an ideal situation. On the other hand, from these figures, it can be seen that though differences exist, the main trends of the system state

Table 1 Quantified results

Control method	Transportation time (s)	First swing angle amplitude (deg)	Second swing angle amplitude (deg)
The proposed method	3.99	1.68	1.20
SMC method	4.28	6.01	7.95
LQR method	4.23	6.13	9.19

trajectories are similar, which shows the effectiveness of the proposed method.

5 Conclusion

In this paper, we propose a global time-optimal trajectory planning method, as well as a tracking controller, for the double pendulum crane system. A series of system constraints, including the permitted amplitudes of double pendulum swing angles, are taken into full consideration when constructing the trajectory. Specifically, the discrete double pendulum crane model is obtained from the original system dynamics, by some linearization and discretization. After that, a time optimization problem is formulated subject to various system constraints, which is equivalent to finding a proper control input sequence. Based on this, the optimization problem is converted into a new formulation, which is proven to be a quasiconvex optimization problem. Then, a bisection-based algorithm is presented to solve this problem and obtain the optimal control input sequence. Utilizing the discrete system model and the obtained control input sequence, we can calculate the corresponding optimal system state trajectories. At last, we design a tracking controller, which can make the trolley track the obtained trajectory properly. Simulation results and experimental results of the proposed method and some comparative methods are included, which show the great performance of our method. In our future work, we will focus on designing feedback control methods to deal with model uncertainties and disturbances, so as to achieve even better performance.

Acknowledgements This work was supported in part by the National Natural Science Foundation of China under Grant 61503200, in part by the Natural Science Foundation of Tianjin under Grant 15JCQNJC03800, and in part by the National Science Fund for Distinguished Young Scholars of China under Grant 61325017.

References

1. Liu, Y., Yu, H.: A survey of underactuated mechanical systems. IET Control Theory Appl. **7**(7), 921–935 (2013)
2. Sun, N., Wu, Y., Fang, Y., Chen, H.: Nonlinear stabilization control of multiple-RTAC systems subject to amplitude restricted actuating torques using only angular position feedback. IEEE Trans. Ind. Electron. **64**(4), 3084–3094 (2017)
3. Sun, N., Wu, Y., Fang, Y., Chen, H., Lu, B.: Nonlinear continuous global stabilization control for underactuated RTAC systems: design, analysis, and experimentation. IEEE/ASME Trans. Mechatron. **22**(2), 1104–1115 (2017)
4. Tuan, L., Lee, S.-G., Dang, V.-H., Moon, S., Kim, B.: Partial feedback linearization control of a three-dimensional overhead crane. Int. J. Control Autom. Syst. **11**(4), 718–727 (2013)
5. Tuan, L., Lee, S.-G., Moon, S.-C.: Partial feedback linearization and sliding mode techniques for 2D crane control. Trans. Inst. Meas. Control **36**(1), 78–87 (2014)
6. Zhang, Z., Wu, Y., Huang, J.: Differential-flatness-based finite-time anti-swing control of underactuated crane systems. Nonlinear Dyn. **87**(3), 1749–1761 (2017)
7. Yang, J., Yang, K.: Adaptive coupling control for overhead crane systems. Mechatronics **17**(2–3), 143–152 (2007)
8. Park, M.-S., Chwa, D., Eom, M.: Adaptive sliding-mode antiswing control of uncertain overhead cranes with high-speed hoisting motion. IEEE Trans. Fuzzy Syst. **22**(5), 1262–1271 (2014)
9. Sun, N., Fang, Y., Chen, H.: Adaptive antiswing control for cranes in the presence of rail length constraints and uncertainties. Nonlinear Dyn. **81**(1), 41–51 (2015)
10. Sun, N., Fang, Y., Zhang, X.: Energy coupling output feedback control of 4-DOF underactuated cranes with saturated inputs. Automatica **49**(5), 1318–1325 (2013)
11. Sun, N., Fang, Y.: New energy analytical results for the regulation of underactuated overhead cranes: an end-effector motion-based approach. IEEE Trans. Ind. Electron. **59**(12), 4723–4734 (2012)
12. Almutairi, N., Zribi, M.: Sliding mode control of a three-dimensional overhead crane. J. Vib. Control **15**(11), 1679–1730 (2009)
13. Xi, Z., Hesketh, T.: Discrete time integral sliding mode control for overhead crane with uncertainties. IET Control Theory Appl. **4**(10), 2071–2081 (2010)
14. Ngo, Q., Hong, K.: Sliding-mode antiswing control of an offshore container crane. IEEE/ASME Trans. Mechatron. **17**(2), 201–209 (2012)

15. Singhose, W., Kim, D., Kenison, M.: Input shaping control of double-pendulum bridge crane oscillations. ASME J. Dyn. Syst. Meas. Control **130**(3), 034504.1–034504.7 (2008)
16. Blackburn, D., Singhose, W., Kitchen, J., Patrangenaru, V., Lawrence, J., Kamoi, T., Taura, A.: Command shaping for nonlinear crane dynamics. J. Vib. Control **16**(4), 477–501 (2010)
17. Daqaq, M., Masoud, Z.: Nonlinear input-shaping controller for quay-side container cranes. Nonlinear Dyn. **45**, 149–170 (2006)
18. Vukov, M., Loock, W., Houska, B., Ferreau, H,. Swevers, J., Diehl, M.: Experimental validation of nonlinear MPC on an overhead crane using automatic code generation. In: Proceedings of American Control Conference, Fairmont Queen Elizabeth, Montral, Canada, pp. 6264–6269 (2012)
19. Chen, H., Fang, Y., Sun, N.: A swing constraint guaranteed MPC algorithm for underactuated overhead cranes. IEEE/ASME Trans. Mechatron. **21**(5), 2543–2555 (2016)
20. Wu, Z., Xia, X., Zhu, B.: Model predictive control for improving operational efficiency of overhead cranes. Nonlinear Dyn. **79**(4), 2639–2657 (2015)
21. Zhao, Y., Gao, H.: Fuzzy-model-based control of an overhead crane with input delay and actuator saturation. IEEE Trans. Fuzzy Syst. **20**(1), 181–186 (2012)
22. Nakazono, K., Ohnishi, K., Kinjo, H., Yamamoto, T.: Load swing suppression for rotary crane system using direct gradient descent controller optimized by genetic algorithm. Trans. Inst. Syst. Control Inf. Eng. **22**(8), 303–310 (2011)
23. Lee, L., Huang, P., Shih, Y., Chiang, T., Chang, C.: Parallel neural network combined with sliding mode control in overhead crane control system. J. Vib. Control **20**, 749–760 (2012)
24. Lee, H.: Motion planning for three-dimensional overhead cranes with high-speed load hositing. Int. J. Control **78**(12), 875–886 (2005)
25. Uchiyama, N., Ouyang, H., Sano, S.: Simple rotary crane dynamics modeling and open-loop control for residual load sway suppression by only horizontal boom motion. Mechatronics **23**(8), 1223–1236 (2013)
26. Sun, N., Fang, Y., Zhang, X., Yuan, Y.: Transportation task-oriented trajectory planning for underactuated overhead cranes using geometric analysis. IET Control Theory Appl. **6**(10), 1410–1423 (2012)
27. Wu, Z., Xia, X.: Optimal motion planning for overhead cranes. IET Control Theory Appl. **8**(17), 1833–1842 (2014)
28. Sun, N., Fang, Y., Zhang, Y., Ma, B.: A novel kinematic coupling-based trajectory planning method for overhead cranes. IEEE/ASME Trans. Mechatron. **17**(1), 166–173 (2012)
29. Chen, H., Fang, Y., Sun, N.: Optimal trajectory planning and tracking control method for overhead cranes. IET Control Theory Appl. **10**(6), 692–699 (2016)
30. Avanço, R.H., Navarro, H.A., Brasil, R.M.L.R.F., Balthazar, J.M., Bueno, Á.M., Tusset, A.M.: Statements on nonlinear dynamics behavior of a pendulum, excited by a crank-shaft-slider mechanism. Meccanica **51**, 1301–1320 (2016)
31. Avanço, R.H., Navarro, H.A., Nabarrete, A., Balthazar, J.M., Tusset, A.M.: Chaotic behavior in the double pendulum under parametric resonance. In: Proceedings of the ASME International Mechanical Engineering Congress and Exposition IMECE2016 (2016)
32. Vaughan, J., Kim, D., Singhose, W.: Control of tower cranes with double-pendulum payload dynamics. IEEE Trans. Control Syst. Technol. **18**(6), 1345–1358 (2010)
33. Singhose, W., Kim, D.: Manipulation with tower cranes exhibiting double-pendulum oscillations. In: Proceedings of 2007 IEEE International Conference on Robotics and Automation, Roma, Italy, pp. 4550–4555 (2007)
34. Masoud, Z., Alhazza, K., Abu-Nada, E., Majeed, M.: A hybrid command-shaper for double-pendulum overhead cranes. J. Vib. Control **20**(1), 24–37 (2014)
35. Sun, N., Fang, Y., Qian, Y.: Motion planning for cranes with double pendulum effects subject to state constraints. Control Theory Appl. **31**(7), 974–980 (2014). **(in Chinese with an English abstract)**
36. Tuan, L., Lee, S.: Sliding mode controls of double-pendulum crane systems. J. Mech. Sci. Technol. **27**(6), 1863–1873 (2013)
37. Sun, N., Fang, Y., Chen, H., Lu, B.: Amplitude-saturated nonlinear output feedback antiswing control for underactuated cranes with double-pendulum cargo dynamics. IEEE Trans. Ind. Electron. **64**(3), 2135–2146 (2017)
38. Boyd, S., Vandenberghe, L.: Convex Optimization. Cambrideg University Press, New York (2004)
39. Grant, M., Boyd, S.: CVX: Matlab software for disciplined convex programming, version 2.0 beta. http://cvxr.com/cvx (2013)
40. Grant, M., Boyd, S.: Graph implementations for nonsmooth convex programs. In: Blondel, V., Boyd, S., Kimura, H. (eds.) Recent Advances in Learning and Control (A Tribute to M. Vidyasagar). Lecture Notes in Control and Information Sciences, pp. 95–110. Springer (2008). http://stanford.edu/~boyd/graph_dcp.html
41. Makkar, C., Hu, G., Sawyer, W., Dixon, W.: Lyapunov-based tracking control in the presence of uncertain nonlinear parameterizable friction. IEEE Trans. Autom. Control **52**(10), 1988–1994 (2007)
42. Sun, N., Fang, Y., Chen, H., He, B.: Adaptive nonlinear crane control with load hoisting/lowering and unknown parameters: design and experiments. IEEE/ASME Trans. Mechatron. **20**(5), 2107–2119 (2015)
43. Huang, C., Wang, W., Chiu, C.: Design and implementation of fuzzy control on a two-wheel inverted pendulum. IEEE Trans. Ind. Electron. **58**(7), 2988–3001 (2011)
44. Herisse, B., Hame, T., Mahony, R., Russotto, F.: Landing a VTOL unmanned aerial vehicle on a moving platform using optical flow. IEEE Trans. Robot. **28**(1), 77–89 (2012)